

RSC Advances



This is an *Accepted Manuscript*, which has been through the Royal Society of Chemistry peer review process and has been accepted for publication.

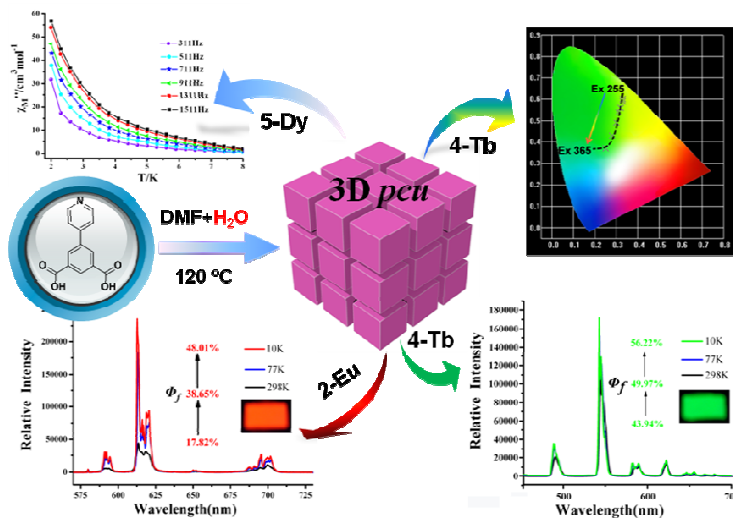
Accepted Manuscripts are published online shortly after acceptance, before technical editing, formatting and proof reading. Using this free service, authors can make their results available to the community, in citable form, before we publish the edited article. This *Accepted Manuscript* will be replaced by the edited, formatted and paginated article as soon as this is available.

You can find more information about *Accepted Manuscripts* in the [Information for Authors](#).

Please note that technical editing may introduce minor changes to the text and/or graphics, which may alter content. The journal's standard [Terms & Conditions](#) and the [Ethical guidelines](#) still apply. In no event shall the Royal Society of Chemistry be held responsible for any errors or omissions in this *Accepted Manuscript* or any consequences arising from the use of any information it contains.

Graphical Abstract

A family of 3D lanthanide organic frameworks with H₂PIP has been synthesized and structurally characterized. The tunable luminescence and slow magnetic relaxation behaviour are investigated.



ARTICLE

A family of 3D lanthanide organic frameworks with tunable luminescence and slow magnetic relaxation

Cite this: DOI: 10.1039/x0xx00000x

Qipeng Li,^{a,b} and Shaowu Du*^a

Received 00th January 2014,
Accepted 00th January 2014

DOI: 10.1039/x0xx00000x

www.rsc.org/

A family of 3D lanthanide organic frameworks with 5-(pyridin-4-yl)isophthalic acid (H₂PIP), formulated as [Ln₂(PIP)₃(H₂O)₄]·2DMF·3H₂O (Ln = Sm **1**, Eu **2**, Gd **3**, Tb **4**, Dy **5** and Ho **6**) have been synthesized and structurally characterized. They are isomorphous and feature a 3D 6-connected *pcu* topology. The tunable luminescence of **2** and **4** is investigated by changing the temperature and the variation of excitation wavelength. In addition, the slow magnetic relaxation behavior is observed in **5**.

Introduction

The design and construction of lanthanide organic frameworks have attracted great interest not only due to their fascinating structures but also because of their potential applications as luminescent and magnetic materials.¹ To date, a large number of lanthanide organic frameworks have been synthesized and their magnetic properties including single-molecule magnets (SMMs) and single-chain magnets (SCMs) have been extensively studied.² Such lanthanide organic frameworks can be constructed by combining the lanthanide ions with various organic linkers under solvothermal conditions. Particularly, the Dy(III) ion has been widely used in the synthesis of molecule-based magnetic framework materials due to its large number of unpaired electrons and the presence of significant uniaxial anisotropy.³ In addition, the luminescent intensity and emission chromaticity of lanthanide organic frameworks can be tuned by varying the temperature and excitation wavelengths.⁴

On the other hand, the selection of organic ligands is very crucial for the synthesis of lanthanide organic frameworks. For example, the multi-carboxylic acid ligands are widely used in the construction of lanthanide organic frameworks owing to their various coordination modes and high affinity of lanthanide ions for the oxygen atom.⁵ So far, a great deal of lanthanide organic frameworks with 1,3-benzenedicarboxylic acid (1,3-H₂BDC) and pyridine-3,5-dicarboxylic acid (3,5-H₂PDC) ligands have been synthesized.^{4a, 6} In comparison, just a few examples of lanthanide organic frameworks constructed by 5-(4-pyridyl)isophthalic acid (H₂PIP), which has one additional

aromatic ring compared to H₂BDC and 3,5-H₂PDC ligands have been reported up to now.⁷

In our present work, we successfully construct a family of 3D lanthanide organic frameworks based on the H₂PIP ligand, formulated as [Ln₂(PIP)₃(H₂O)₄]·2DMF·3H₂O (Ln = Sm **1**, Eu **2**, Gd **3**, Tb **4**, Dy **5** and Ho **6**), which are isomorphous and both display a 3D 6-connected *pcu* topology. Our results showed that the luminescence of **2** and **4** could be tuned by changing the temperature and the excitation wavelength. Furthermore, the slow magnetic relaxation behavior is observed in **5**.

Experimental

Materials and methods

All the starting materials and solvents were available commercially sources and used as purchased without further purification. Thermogravimetric experiments were performed using a TGA/NETZSCH STA-449C instrument heated from 30-1000°C (heating rate of 10°C/min, nitrogen stream). IR spectra using KBr pellets were recorded on a Spectrum-One FT-IR spectrophotometer. The powder X-ray diffraction (XRD) patterns were recorded on crushed single crystals in the 2θ range 5-50° using Cu-Kα radiation. Element analyses for C, H and N were measured with an Elemental Vairo ELIII analyzer. Fluorescence spectra for the solid samples were performed on an Edinburgh Analytical instrument FLS920. The magnetic susceptibility data were collected on Quantum Design MPMS (SQUID)-XL magnetometer and PPMS-9T system.

Synthesis of $[\text{Ln}_2(\text{PIP})_3(\text{H}_2\text{O})_4] \cdot 2\text{DMF} \cdot 3\text{H}_2\text{O}$ ($\text{Ln} = \text{Sm } \mathbf{1}$, $\text{Eu } \mathbf{2}$, $\text{Gd } \mathbf{3}$, $\text{Tb } \mathbf{4}$, $\text{Dy } \mathbf{5}$ and $\text{Ho } \mathbf{6}$).

H_2PIP (0.5 mmol) and $\text{Sm}(\text{NO}_3)_3 \cdot 6\text{H}_2\text{O}$ (0.25 mmol) were placed in a 20mL of Teflon-lined stainless steel vessel with 10mL of DMF / H_2O (V/V = 1:1). The mixtures were heated to 120 °C in 4 h and kept at this temperature for three days, and then cooled to room temperature during another two days. Pink crystals of **1** were obtained in 60% yield based on $\text{Sm}(\text{NO}_3)_3 \cdot 6\text{H}_2\text{O}$. Elemental anal. calcd. for **1** $\text{Sm}_2\text{C}_{45}\text{H}_{50}\text{N}_5\text{O}_{22}$ (%): C, 41.15; N, 5.33; H, 3.84. Found (%): C, 41.40; H, 3.87; N, 5.23. IR (KBr, cm^{-1}): 3360 s, 3053 vw, 2928 vw, 1872 vw, 1660 s, 1550 w, 1429 m, 1300 w, 1099.5 vw, 1005 m, 936.2 m 878 w, 827.0 s, 781.6 w, 715 w, 634.2 m.

Colorless crystals of **2-5** and pink crystals of **6** were obtained in moderate yields (49-66%) by a similar method as described for **1** except that the corresponding $\text{Ln}(\text{NO}_3)_3 \cdot 6\text{H}_2\text{O}$ salts were used instead of $\text{Sm}(\text{NO}_3)_3 \cdot 6\text{H}_2\text{O}$. Elemental anal. calcd. for **2** $\text{Eu}_2\text{C}_{45}\text{H}_{50}\text{N}_5\text{O}_{22}$ (%): C, 41.05; H, 3.83; N, 5.32. Found (%): C, 41.40; H, 3.78; N, 5.43. IR (KBr, cm^{-1}): 3382.3 s, 3065.3 w, 2928.6 w, 1815.2 w, 1663.3 vw, 1500.9 w, 1440.2 vw, 1298.7 w, 1255.7 w, 1099.5 w, 1068.9 vw, 1007.4 w, 932.1 vw, 876.7 m, 826.8 s, 781.7 s, 716.5 m, 666.5 m, 643.9 s. Elemental anal. calcd. for **3** $\text{Gd}_2\text{C}_{45}\text{H}_{50}\text{N}_5\text{O}_{22}$ (%): C, 40.72; N, 5.28; H, 3.80. Found (%): C, 40.38; H, 3.87; N, 5.25. IR (KBr, cm^{-1}): 3360 s, 3060 vw, 2914 vw, 1869 vw, 1665 s, 1552 w, 1442 m, 1305 w, 1100.8 vw, 1007 m, 937 m 879 w, 827 s, 785 w, 717 w, 636 m. Elemental anal. calcd. for **4** $\text{Tb}_2\text{C}_{45}\text{H}_{50}\text{N}_5\text{O}_{22}$ (%): C, 40.62; H, 3.79; N, 5.26. Found (%): C, 40.40; H, 3.87; N, 5.23. IR (KBr, cm^{-1}): 3383.8 s, 3065.7 vw, 2928.6 vw, 1944.1 w, 1869.2 vw, 1666.5 w, 1552.3 vw, 1507.9 w, 1440.6 w, 1299.5 m, 1225.6 m, 1174.9 w, 1099.8 m, 1007.7 m, 936.6 w, 877.7 w, 781.6 s, 716.4 s, 667.2 m, 635.3 s, 571.8 m, 513.3 w. Elemental anal. calcd. for **5** $\text{Dy}_2\text{C}_{45}\text{H}_{50}\text{N}_5\text{O}_{22}$ (%): C, 40.12; N, 3.68; H, 5.47. Found (%): C, 40.40; H, 3.77; N, 5.23. IR (KBr, cm^{-1}): 3381 s, 3065 vw, 2928 vw, 1869 vw, 1658 s, 1552 w, 1439 m, 1300 w, 1099.8 vw, 1007 m, 936.6 m 877.7 w, 827.0 s, 781.6 w, 716.4 w, 635.3 m. Elemental anal. calcd. for **6** $\text{Ho}_2\text{C}_{45}\text{H}_{50}\text{N}_5\text{O}_{22}$ (%): C, 40.23; N, 5.22; H, 3.75. Found (%): C, 40.12; H, 3.79; N, 5.25. IR (KBr, cm^{-1}): 3392 s, 3058 vw, 2910 vw, 1860 vw, 1658 s, 1545 w, 1445 m, 1300 w, 1099 vw, 1007 m, 938 m 877.8 w, 827 s, 783 w, 716.8 w, 635.6 m.

Crystal Structure Determination

Single-crystal X-ray diffraction data were collected on a Rigaku Diffractometer with a Mercury CCD area detector (Mo $\text{K}\alpha$; $\lambda = 0.71073 \text{ \AA}$) at room temperature. Empirical absorption corrections were applied to the data using the Crystal Clear program.⁸ The structures were solved by the direct method and refined by the full-matrix least-squares on F^2 using the SHELXTL-97 program.⁹ Metal atoms in each compounds were located from the E -maps and other non-hydrogen atoms were located in successive difference Fourier syntheses. All non-hydrogen atoms were refined anisotropically and the hydrogen atoms were positioned geometrically. The hydrogen atoms of coordinated water and lattice water molecules were not added.

The PIP^{2-} ligand and coordinated water molecule in **1** are both positional disordered and have been treated as two equal parts. Some lattice water molecules in **1** are also disordered.¹⁰ The crystal data of **1-6** all existed severe disordered problems, thus only the refinement of crystal data of **1** and **5** were provided. Crystallographic data and other pertinent information for **1** and **5** are summarized in Table 1. Selected bond lengths and angles for **1** and **5** are listed in Table S1† and S2†. CCDC numbers are 1010482 for **1** and 958686 for **5**, respectively.

Table 1 Crystal Data and Structure Refinement of **1** and **5**

Compounds	1	5
CCDC	1010482	958686
Formula	$\text{C}_{45}\text{H}_{50}\text{N}_5\text{O}_{22}\text{Sm}_2$	$\text{C}_{45}\text{H}_{50}\text{N}_5\text{O}_{22}\text{Dy}_2$
Mr	1313.60	1337.90
Space group	$P2_1/c$	$P2_1/c$
a (Å)	13.472(6)	13.405(3)
b (Å)	14.814(7)	14.705(4)
c (Å)	13.413 (8)	13.388(3)
α (deg)	90	90
β (deg)	99.14(3)	99.34(4)
γ (deg)	90	90
V (Å ³)	2642.9(2)	2603.9(1)
Z	2	2
D_c (g cm ⁻³)	1.630	1.686
M (mm ⁻¹)	2.28	2.93
$F(000)$	1278	1326
GOF	1.09	1.05
R_1^a	0.041	0.032
wR_2^a	0.099	0.075

$$^a R = \sum (||F_o| - |F_c||) / \sum |F_o|, wR = \{ \sum w[(F_o^2 - F_c^2)^2] / \sum w[(F_o^2)^2] \}^{1/2}$$

Results and Discussion

Synthesis and description of Crystal Structures

A family of 3D lanthanide organic frameworks with H_2PIP ligand, namely $[\text{Ln}_2(\text{PIP})_3(\text{H}_2\text{O})_4] \cdot 2\text{DMF} \cdot 3\text{H}_2\text{O}$ ($\text{Ln} = \text{Sm } \mathbf{1}$, $\text{Eu } \mathbf{2}$, $\text{Gd } \mathbf{3}$, $\text{Tb } \mathbf{4}$, $\text{Dy } \mathbf{5}$ and $\text{Ho } \mathbf{6}$) have been successfully prepared by the hydrothermal reaction of $\text{Ln}(\text{NO}_3)_3 \cdot 6\text{H}_2\text{O}$ and H_2PIP in the mixed-solvent of DMF/ H_2O (V/V = 1:1). Compounds **1-6** are isomorphous which is confirmed by XRD, TGA, IR, Elemental analysis and lattice parameters. Herein, only the structure of **1** is discussed in detail.

Compound **1** crystallizes in the monoclinic space group $P2_1/c$ and its asymmetric unit contains one Sm(III) ion, one and a half PIP^{2-} ligands, two coordinated water molecules, one guest DMF and one and a half lattice water molecules. The Sm(III) center is nine-coordinated by seven carboxylate O atoms from five different PIP^{2-} ligands and two O atoms from two different coordinated water molecules (Fig 1a). The PIP^{2-} ligands in **1** display $(\kappa^1-\kappa^1)-(\kappa^2-\mu_2)-\mu_4$ and $(\kappa^2)-(\kappa^2)-\mu_2$ coordination modes, respectively (Scheme S1).

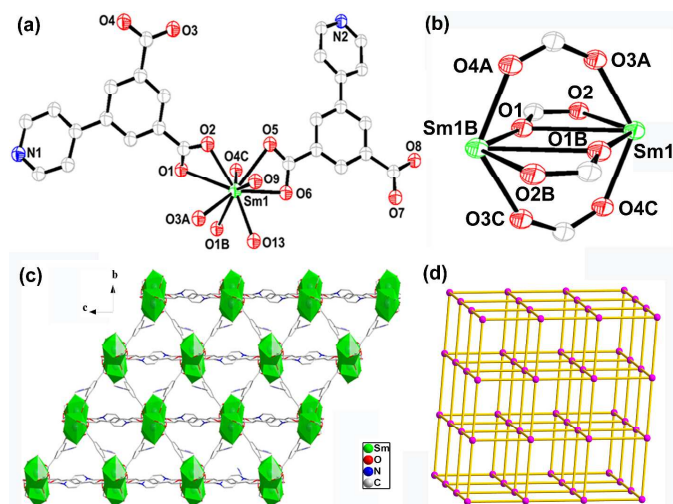


Fig 1 (a) View of the coordination environment of the Sm(III) ions in **1**. Symmetry codes: A $x, -y+1/2, z-1/2$; B $-x, -y+1, -z+1$; C $-x, y+1/2, -z+3/2$. (b) The binuclear $\{\text{Sm}_2(\text{CO}_2)_4\}$ units. (c) The polyhedral and packing views for the 3D framework of **1**. (d) The 6-connected *pcu* topological net of **1**.

In addition, two equivalent Sm(III) ions are bridged by four carboxylates *via* bridging bidentate and tridentate arrangements to generate a $\{\text{Sm}_2(\text{CO}_2)_4\}$ unit with the Sm...Sm distance of 4.117 Å (Fig 1b). Such dinuclear units act as secondary building units (SBUs) which are expanded into a 1D chain through carboxylates. These chains are further extended into a 2D layer network and 3D frameworks *via* the carboxylates of PIP^{2-} ligands (Fig 1c). From the topological point of view, the PIP^{2-} ligands can be defined as a connector and the dinuclear $\{\text{Sm}_2(\text{CO}_2)_4\}$ units can be simplified as a six-connected node. Therefore **1** can be abstracted into a 6-connected network with the *Schläfli* symbol of $\{4^4 12.6^3\}$, which is a typical *pcu* topological net (Fig 1d).¹¹

XRD patterns and thermal properties

The powder XRD of **1-6** are performed at room temperature to characterize their purity (Fig S1). All the diffraction peak positions on the curves correspond well with the simulated XRD patterns, indicating the phase purity of the as-synthesized samples. The thermo-gravimetric analysis (TGA) experiments of **1-6** are conducted in the temperature range of 30-1000°C under a flow of nitrogen with the heating rate of 10°C min⁻¹. The TGA curves of **1-6** are very similar and **1** has a weight loss of 20.55% from 40 to 400°C, which is assigned to the release of three guest water and two DMF and four coordinated water molecules (calcd. 20.34%). Then the framework begins to decompose upon further heating (Fig S2).

Tunable luminescence

The free H_2PIP ligand presented an emission with the band peaking around 459 nm upon excitation at 394 nm (Fig. S3). Upon excitation at 280 nm, the characteristic emissions of **2** are observed in the range of 570–720 nm. The typical emission peaks are associated with the $4f \rightarrow 4f$ transitions of the $^5\text{D}_0$ excited state to the low-lying $^7\text{F}_j$ ($J = 0-4$) levels. Note that the $^5\text{D}_0 \rightarrow ^7\text{F}_2$ transition of Eu(III) centered at

614 nm for **2** (Fig S4).⁴ When it's excited at 310 nm, the emission spectrum of **4** displays green luminescence with the typical emission peaks at 488, 543, 582 and 621 nm, which are assigned to $^5\text{D}_4 \rightarrow ^7\text{F}_j$ ($J = 6-3$) transitions (Fig S5).

The quantum yields measured at 298, 77 and 10 K are 17.82, 38.6 and 48.01% for **2** (at $\lambda_{\text{ex}} = 280$ nm) and 43.94, 49.97 and 56.22% for **4** (at $\lambda_{\text{ex}} = 310$ nm), respectively (Fig 2a and Fig 3a). These results reveal that the quantum yields of **2** and **4** increase gradually with dropping temperature, which may be due to the reduction of molecular thermal vibration at low temperatures.^{12, 7b} The corresponding lifetime at 298 K for **2** is *ca.* 0.3911 ms, while that for **4** is *ca.* 0.8372 ms (Table S3). The luminescence decay curves of **2** and **4** are determined by monitoring $^5\text{D}_0 \rightarrow ^7\text{F}_2$ line excited at 280 nm and $^5\text{D}_4 \rightarrow ^7\text{F}_5$ line excited at 310 nm, respectively.

The emission intensity of $^5\text{D}_0 \rightarrow ^7\text{F}_2$ in **2** gradually increases with the excitation wavelength varied from 255 to 285 nm, but gradually decreases with the excitation wavelength varied from 295 to 365 nm (Fig 2b). As a result, the emission of **2** varies from light-yellow to red and then to orange, as illustrated by the CIE-1931 chromaticity diagram (Fig 2c). A similar situation occurs with the emission intensity of $^5\text{D}_4 \rightarrow ^7\text{F}_5$ in **4**. As the excitation wavelength varies from 255 to 365 nm, the emission of **4** changes from yellow-green to yellowish green, and then to green (Fig 3b and 3c).

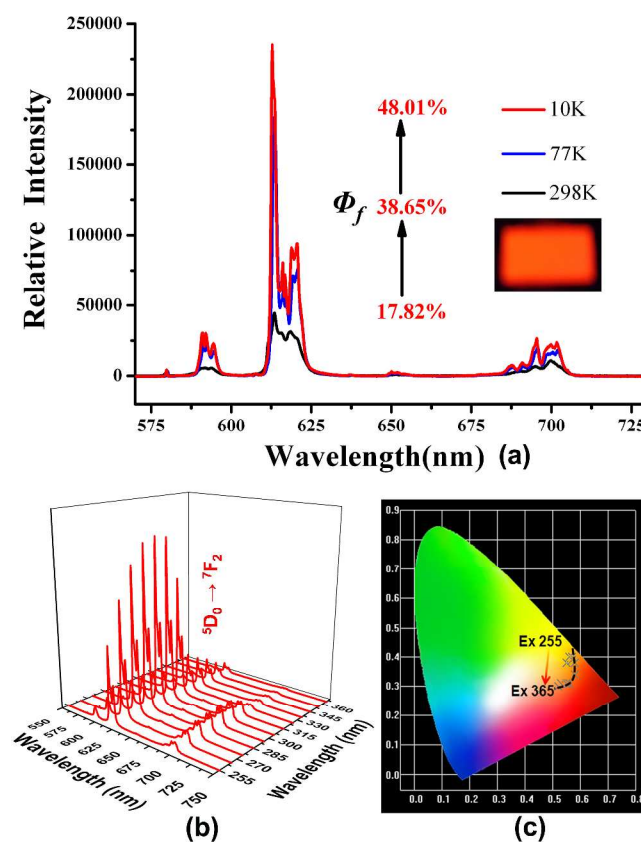


Fig 2 (a) Relative emission spectra of **2** with the variation of their quantum yields in the solid state at 10, 77 and 298 K. (b) The emission spectra of **2** by varying the excitation light under the same metrical conditions. (c) The CIE-1931 chromaticity diagram show the emissions varying from the light yellow to red and then to orange for **2** by changing the excitation wavelength.

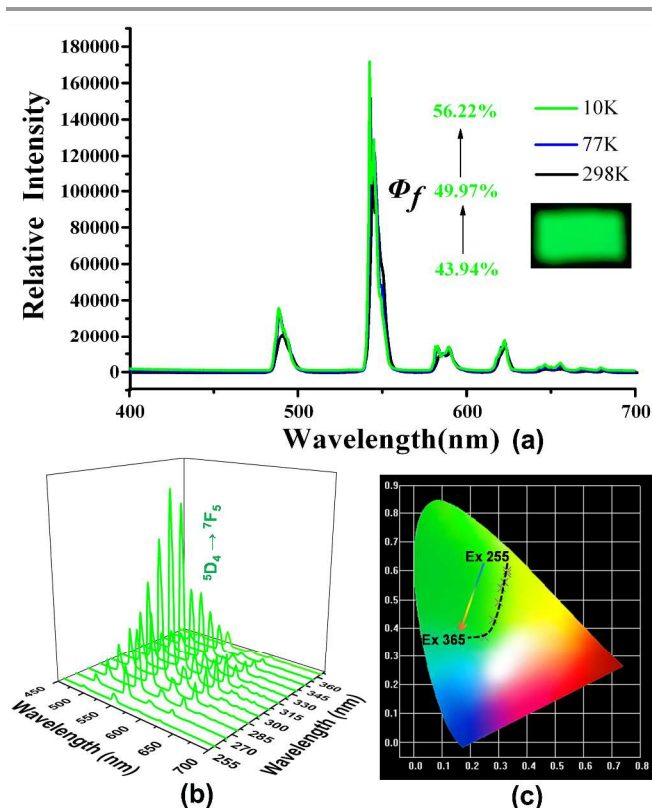


Fig 3 (a) Relative emission spectra of **4** with the variation of their quantum yields in the solid state at 10, 77 and 298 K. (b) The emission spectra of **4** by varying the excitation light under the same metrical conditions. (c) The CIE-1931 chromaticity diagram of **4** showing the emissions from yellow-green to yellowish green and then to green by changing the excitation wavelength.

Magnetic properties

Temperature-dependent magnetic susceptibility measurements of **5** and **6** have been carried out in an applied magnetic field of 1000 Oe in the temperature range 300–2 K. The $\chi_M T$ value of **5** at 300 K is $28.73 \text{ cm}^3 \text{ K mol}^{-1}$, which is very close to the value of $28.33 \text{ cm}^3 \text{ K mol}^{-1}$ for two uncoupled Dy(III) ions ($S = 5/2$, $L = 5$, $^6H_{15/2}$ and $g = 4/3$).¹³ The $\chi_M T$ product gradually decreases

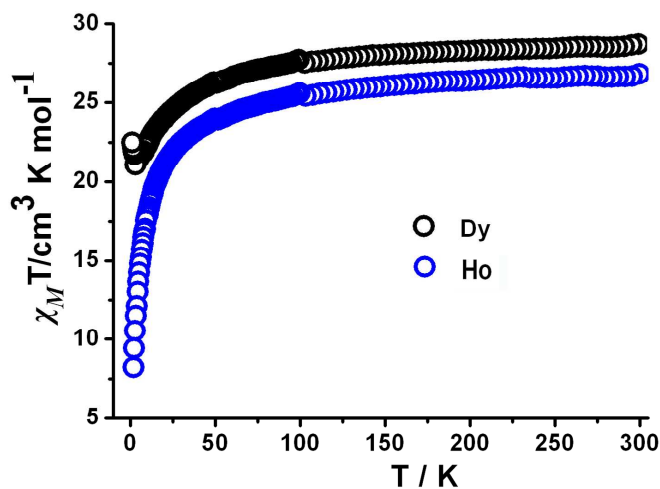


Fig 4 Temperature dependence of $\chi_M T$ values for **5** and **6**.

with the temperature to reach a minimum of $21.09 \text{ cm}^3 \text{ K mol}^{-1}$ at 3.91 K, which is mainly ascribed to the progressive depopulation of excited Stark sublevels (Fig 4). At low temperatures, the $\chi_M T$ product increases up to $22.50 \text{ cm}^3 \text{ K mol}^{-1}$ at 2 K, which obviously suggests the presence of weak ferromagnetic interactions between Dy(III) ions as observed in other dinuclear Dy(III) systems.¹⁴ In addition, the temperature dependent χ_M^{-1} value above 10 K obeys the Curie-Weiss law with $C = 28.7 \text{ cm}^3 \text{ K mol}^{-1}$ and $\theta = -4.67 \text{ K}$ (Fig S6).

At room temperature, the $\chi_M T$ value is $24.46 \text{ cm}^3 \text{ K mol}^{-1}$ for **6**, which is lower than $28.15 \text{ cm}^3 \text{ K mol}^{-1}$ for two independent Ho(III) (5I_8 and $g = 5/4$).¹⁵ Below 50 K, the $\chi_M T$ value decreases smoothly to reach a minimal value of $8.30 \text{ cm}^3 \text{ K mol}^{-1}$ at 2 K (Fig 4). This feature indicates anti-ferromagnetic interactions between Ho(III) ions. This tendency can be explained by the spin orbital coupling of Ho-MOFs, which leads to the splitting of 4f_n configuration into 7F_6 states and finally into Stark components under the ligand field perturbation.¹⁵ Above 10 K, the magnetic data was fitted by Curie-Weiss equation to give a Curie constant $C = 27.30 \text{ cm}^3 \text{ mol}^{-1}$ and Weiss temperature $\theta = -6.10 \text{ K}$ (Fig S7). The negative θ value indicates the presence of anti-ferromagnetic interactions between the Ho(III) ions.

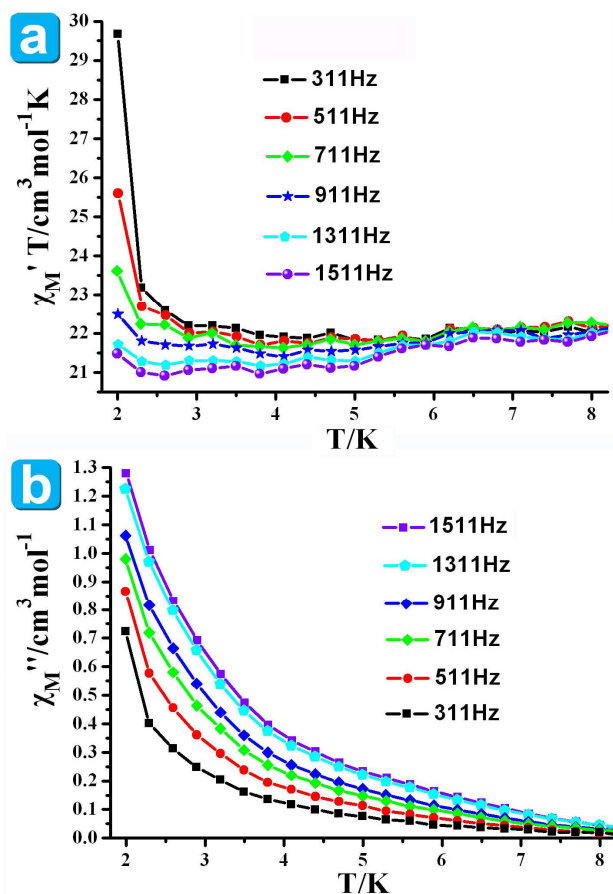


Fig 5. AC susceptibility measured in zero dc fields and plotted as $\chi' T$ vs. T (a) and χ'' vs. T (b) for **5**.

In the M vs. H/T plot of **5**, the M values show a rapid increase in the magnetization at low field and the maximum value is $14.96 N\beta$ at 2 K and 7 T (Fig S8), which is lower than $20 N\beta$ for two Dy(III) ions. It is likely that the anisotropy and crystal-field effect at the Dy(III) ion eliminate the 16-fold degeneracy of the ${}^6H_{15/2}$ ground state.¹⁶ The absence of saturation on the M vs. H data at 2 K suggests the presence of significant anisotropy and low-lying excited states.

In order to understand the dynamics of magnetization, the ac susceptibility measurements of **5** were carried out in a zero-applied dc field with 3 Oe ac field oscillating at the indicated frequencies (311-1511 Hz) under the temperature range of 2-8 K (Fig 5). Both in-phase ($\chi''T$) and out-of-phase (χ'') signals display frequency dependence below 8 K, which suggest the slow magnetization (M) relaxation behavior.¹⁷

Conclusions

A family of new 3D lanthanide organic frameworks constructed by H_2PIP have been synthesized and structurally characterized, which are isomorphous and each features a 3D 6-connected *pcu* topology. It has been observed that the luminescent quantum yields of **2** and **4** increase with the decreasing of temperature and their emissions can be tuned by altering the excitation wavelength. In addition, the slow magnetic relaxation behavior is observed in **5**.

Acknowledgements

This work was supported by the National Basic Research Program of China (973 Program, 2012CB821702), the National Natural Science Foundation of China (21233009 and 21173221) and the State Key Laboratory of Structural Chemistry, Fujian Institute of Research on the Structure of Matter, Chinese Academy of Sciences.

Notes and references

^a State Key Laboratory of Structural Chemistry, Fujian Institute of Research on the Structure of Matter, Chinese Academy of Sciences, Fuzhou, Fujian 350002, P. R. China. E-mail: swdu@fjirsm.ac.cn; Fax: (+86) 591 83709470

^b University of Chinese Academy of Sciences, Beijing 100039, P. R. China.

†Electronic Supplementary Information (ESI) available: Additional figures, IR, TGA and XRD pattern. CCDC: 1010482 for **1** and 958686 for **5**. For ESI and crystallographic data in CIF or other electronic format see DOI: 10.1039/b000000x/.

- (a) M. D. Allendorf, C. A. Bauer, R. K. Bhakta and R. J. T. Houka, *Chem. Soc. Rev.*, **2009**, 38, 1330; (b) A. J. Tasiopoulos, A. Vinslava, W. Wernsdorfer, K. A. Abboub and G. Christou, *Angew. Chem. Int. Ed.*, **2004**, 43, 2117; (c) Y. J. Cui, Y. F. Yue, G. D. Qian and B. L. Chen, *Chem. Rev.*, **2012**, 112, 1126; (d) M. Kurmoo, *Chem. Soc. Rev.*, **2009**, 38, 1353; (e) H. L. Sun, Z. M. Wang and S. Gao, *Coord. Chem. Rev.*, **2010**, 254, 1081; (f) J. Xie, H. M. Shu, Z. X. Han, S. S. Shen, F. Yuan, M. L. Yang, F. X. Dong and G. L. Xue, *ChemPlusChem*, **2014**, 79, 985.
- (a) M. T. Gamer, Y. Lan, P. W. Roesky, A. K. Powell and R. Cle'rac, *Inorg. Chem.*, **2008**, 47, 6581; (b) H. S. Ke, G. F. Xu, Y. N. Guo, P. Gamez, C. M. Beavers, S. J. Teat and J. K. Tang, *Chem. Commun.*, **2010**, 46, 6057; (c) B. Hussain, D. Savard, T. J. Burchell, W. Wernsdorfer and M. Murugesu, *Chem. Commun.*, **2009**, 1100; (d) J. D. Rinehart and J. R. Long, *Chem. Sci.*, **2011**, 2, 2078; (e) T. A. Hudson, K. J. Berry, B. J. Moubaraki, K. S. Murray and R. Robson, *Inorg. Chem.*, **2006**, 45, 549; (f) A. S. R. Chesman, D. R. Turner, B. Moubaraki, K. S. Murray, G. B. Deacon and S. R. Batten, *Chem. Eur. J.*, **2009**, 15, 5203.
- (a) L. Bogani, C. Sangregorio, R. Sessoli and D. Gatteschi, *Angew. Chem., Int. Ed.*, **2005**, 44, 5817; (b) K. Bernot, L. Bogani, A. Caneschi, D. Gatteschi and R. Sessoli, *J. Am. Chem. Soc.*, **2006**, 128, 7947; (c) J. Rocha, L. D. Carlos, F. A. Paz and D. Ananias, *Chem. Soc. Rev.*, **2011**, 40, 926; (d) H. S. Ke, P. Gamez, L. Zhao, G. F. Xu, S. F. Xue and J. K. Tang, *Inorg. Chem.*, **2010**, 49, 7549; (d) R. Sessoli, A. K. Powell, *Coord. Chem. Rev.*, **2009**, 253, 2328; (e) D. N. Woodruff, REP. Winpenny and R. A. Layfield, *Chem. Rev.*, **2013**, 113, 5110; (f) Y. N. Guo, L. Ungur, G. E. Granroth, A. K. Powell, C. J. Wu, S. E. Nagler, J. K. Tang, L. F. Chibotaru, D. M. Cui, *Sci. Rep.*, **2014**, 4, 5471; (g) S. Y. Lin, W. Wernsdorfer, L. Ungur, A. K. Powell, Y. N. Guo, J. K. Tang, L. Zhao, L. F. Chibotaru and H. J. Zhang, *Angew. Chem. Int. Ed.*, **2012**, 51, 12767; (h) P. Zhang, Y. N. Guo, J. K. Tang, *Coord. Chem. Rev.*, **2013**, 257, 1728.
- (a) H. B. Zhang, L. J. Zhou, J. Wei, Z. H. Li, P. Lin and S. W. Du, *J. Mater. Chem.*, **2012**, 22, 21210; (b) H. B. Zhang, X. C. Shan, Z. J. Ma, L. J. Zhou, M. J. Zhang, P. Lin, S. M. Hu, E. Ma, R. F. Li and S. W. Du, *J. Mater. Chem. C.*, **2014**, 2, 1367; (c) L. Wang, E. Yang, H. B. Zhang and J. Zhang, *ChemPlusChem*, **2014**, 79, 1080.
- (a) L. P. Zhang, Y. H. Wan and L. P. Jin, *Polyhedron.*, **2003**, 22, 981; (b) L. Pan, E. B. Woodlock, X. T. Wang and C. Zheng, *Inorg. Chem.*, **2000**, 39, 4174; (c) J. G. Wang, C. C. Huang, X. H. Huang and D. S. Liu, *Cryst. Growth Des.*, **2008**, 8, 795; (d) Q. P. Li, C. B. Tian, H. B. Zhang, J. J. Qian and S. W. Du, *CrystEngComm*, **2014**, 16, 9208; (e) T. Devic, C. Serre, N. Audebrand, J. Marrot and G. Férey, *J. Am. Chem. Soc.*, **2005**, 127, 12788; (f) Q. P. Li and J. J. Qian, *RSC Adv.*, **2014**, 4, 32391; (g) S. Muniappan, S. Lipstman, S. George and I. Goldberg, *Inorg. Chem.*, **2007**, 46, 5544; (h) Q. P. Li, X. Jiang and S. W. Du, *RSC Advances.*, **2015**, 5, 1785; (i) R. Wang, and Z. Zheng, (2010) Rare Earth Complexes with Carboxylic Acids, Polyaminopolycarboxylic Acids, and Amino Acids, in Rare Earth Coordination Chemistry: Fundamentals and Applications (ed C. Huang), John Wiley & Sons, Ltd, Chichester, UK. doi: 10.1002/9780470824870.ch3, 91.
- (a) Y. H. Wan, L. P. Zhang, L. P. Jin, S. Gao and S. Z. Lu, *Inorg. Chem.*, **2003**, 42, 4985; (b) Y. H. Wan, L. P. Zhang and L. P. Jin, *J. Mol. Struct.*, **2003**, 658; (c) B. L. Chen, L. B. Wang and G. D. Qian, *Angew. Chem. Int. Ed.*, **2009**, 48, 500; (d) Y. H. Zhao, Z. M. Su, Y. M. Fu, K. Z. Shao, P. Li, Y. Wang, X. R. Hao, D. X. Zhu and S. D. Liu, *Polyhedron.*, **2008**, 27, 583; (e) J. L. Yi, Z. Y. Fu and S. J. Liao, *J. Coord. Chem.*, **2009**, 14, 2290; (f) Y. Y. Lv, Y. Qi, L. X. Sun, F. Luo, Y. X. Che and J. M. Zheng, *Eur. J. Inorg. Chem.*, **2010**, 5592; (g) Y. T. Liu, Y. Q. Du, X. Wu, Z. P. Zheng, X. M. Lin, L. C. Zhu and Y. P. Cai, *CrystEngComm.*, **2014**, 16, 6797.
- (a) J. Huang, H. M. Li, J. Y. Zhang and C. Y. Su, *Inorg. Chim. Acta.*, **2012**, 388, 16; (b) X. T. Rao, T. Song, B. L. Chen and G. D. Qian, *J. Am. Chem. Soc.*, **2013**, 135, 15559; (c) Q. F. Zhang, F. L. Hu, S. N. Wang and J. M. Dou, *Aust. J. Chem.*, **2012**, 65, 524; (d) Y. G. Sun, J. Li, K. L. Li, Z. H. Xu, F. Ding, B. Y. Ren, S. J. Wang, L. X. You, G. Xiong and P. F. Smet, *CrystEngComm.*, **2014**, 16, 1777; (e) Q. P. Li and S. W. Du, *RSC Adv.*, **2014**, 4, 30963; (f) T. Song, X.T. Rao, Y. J. Cui, Y. Yang and G. D. Qian, *J Alloy Compd.*, **2013**, 555, 22.
- CrystalClear, version 1.36*, Molecular Structure Corp and Rigaku Corp., The Woodlands, TX, and Tokyo, Japan, **2000**.
- G. M. Sheldrick, *SHELXS 97, Program for Crystal Structure Solution*; University of Göttingen: Göttingen, Germany, **1997**.
- Q. P. Li, J. J. Qian, C. B. Tian, P. Lin, Z. Z. He, N. Wang, J. N. Shen, H. B. Zhang, T. Chu, Y. Yang, L. P. Xue and S. W. Du, *Dalton Trans.*, **2014**, 43, 3238.

ARTICLE

11. (a) J. R. Li, Y. Tao, Q. Yu and X. H. Bu, *Chem. Commun.*, 2007, 1527; (b) J. Y. Zou, W. Shi, J. Y. Zhang, Y. F. He, H. L. Gao, J. Z. Cui and P. Cheng, *CrystEngComm.*, **2014**, 16, 7133.
12. (a) Z. H. Weng, D. C. Liu, Z. L. Chen, H. H. Zou, S. N. Qin and F. P. Liang, *Cryst. Growth. Des.*, **2009**, 9, 4163; (b) Y. J. Cui, H. Xu, Y. F. Yue, Z. Y. Guo, J. C. Yu, Z. X. Chen, J. K. Gao, Y. Yu, G. D. Qian and B. L. Chen, *J. Am. Chem. Soc.*, **2012**, 134, 3979.
13. Y. Ma, G. F. Xu, X. Yang, L. C. Li, J. K. Tang, S. P. Yan, P. Cheng and D. Z. Liao, *Chem. Commun.*, **2010**, 46, 8264.
14. P. H. Lin, T. Burchell, R. Cle'ac and M. Murugesu, *Angew. Chem., Int. Ed.*, **2008**, 47, 8848.
15. H. B. Zhang, C. B. Tian, S. T. Wu, J. D. Lin, Z. H. Li and S. W. Du, *J. Mol. Struct.*, **2011**, 355.
16. (a) G. F. Xu, Q. L. Wang, P. Gamez, J. K. Tang, S. P. Yan, P. Cheng and D. Z. Liao, *Chem. Commun.*, **2010**, 46, 1506; (b) J. Tang, I. Hewitt, N. T. Madhu, G. Chastanet, W. Wernsdorfer, C. E. Anson, C. Benelli, R. Sessoli and A. K. Powell, *Angew. Chem. Int. Ed.*, **2006**, 45, 1729.
17. (a) Y. L. Hou, G. Xiong, B. Shen, B. Zhao, Z. Chen and J. Z. Cui, *Dalton Trans.*, **2013**, 42, 3587; (b) Z. R. Jhu, C. I. Yang and G. H. Lee, *CrystEngComm.*, **2013**, 15, 2456; (c) X. L. Liu, X. Wang, T. Gao, Y. Xu, X. Shen and D. R. Zhu, *CrystEngComm.*, **2014**, 16, 2779; (c) Y. L. Hou, R. R. Cheng, G. Xiong, J. Z. Cui and B. Zhao, *Dalton Trans.*, **2014**, 43, 1814; (d) X. H. Wei, L. Y. Yang, S. Y. Liao, M. Zhang, J. L. Tian, R. Y. Du and X. Liu, *Dalton Trans.*, **2014**, 43, 5793; (e) Y. Peng, C. B. Tian, Y. H. Lan, N. Magnani, Q. P. Li, H. B. Zhang, A. K. Powell and S. W. Du, *Eur. J. Inorg. Chem.*, **2013**, 5534; (f) Y. N. Guo, G. F. Xu, Y. Guo and J. K. Tang, *Dalton Trans.*, **2011**, 40, 9953; (g) L. Ungur, S. Y. Lin, J. K. Tang and L. F. Chibotaru, *Chem. Soc. Rev.*, **2014**, 43, 6894; (h) P. Zhang, L. Zhang, C. Wang, S. F. Xue, S. Y. Lin and J. K. Tang, *J. Am. Chem. Soc.*, **2014**, 136, 4484.